Sussex Research Online

The Baryon asymmetry in the standard model with a low cut-off

Article (Published Version)

http://sro.sussex.ac.uk

The baryon asymmetry in the standard model with a low cut-off

Dietrich Bödeker,[a] **Lars Fromme,**[a] **Stephan J. Huber**[b] **and Michael Seniuch**[a]

[a]*Fakultät für Physik, Universität Bielefeld, D-33615 Bielefeld, Germany*
[b]*Theory Division, Physics Department, CERN, CH-1211 Geneva 23, Switzerland*
 E-mail: `bodeker@physik.uni-bielefeld.de`, `fromme@physik.uni-bielefeld.de`,
 `stephan.huber@cern.ch`, `seniuch@physik.uni-bielefeld.de`

ABSTRACT: We study the generation of the baryon asymmetry in a variant of the standard model, where the Higgs field is stabilized by a dimension-six interaction. Analyzing the one-loop potential, we find a strong first order electroweak phase transition for Higgs masses up to at least 170 GeV. Dimension-six operators induce also new sources of CP violation. We compute the baryon asymmetry in the WKB approximation. Novel source terms in the transport equations enhance the generated baryon asymmetry. For a wide range of parameters the model predicts a baryon asymmetry close to the observed value.

KEYWORDS: Cosmology of Theories beyond the SM, Baryogenesis.

Contents

1. Introduction

The baryon asymmetry of the universe has recently been determined to an unprecedented accuracy,

$$\eta_B \equiv \frac{n_B}{s} = (8.9 \pm 0.4) \times 10^{-11}, \tag{1.1}$$

by combining measurements of the cosmic microwave background [1] and large scale structures [2]. Explaining its origin is one of the great challenges of modern particle physics and cosmology. For baryogenesis Sakharov's three conditions, B violation, CP violation and deviation from thermal equilibrium have to be satisfied. In principle these conditions could be met within the standard model (SM) at the electroweak phase transition (EWPT) [3]. A more quantitative analysis shows however that the baryon asymmetry cannot be explained within the SM because there is not enough CP violation [4] and the phase transition turns into a smooth crossover for Higgs masses $m_H \gtrsim 80\,\mathrm{GeV}$ [5]. In fact, electroweak baryogenesis requires an even stronger criterion to be satisfied: The Higgs vacuum expectation value (vev) at the critical temperature, $v_c \equiv \langle \phi(T_c) \rangle$, must be larger than about T_c in order to avoid baryon number washout after the phase transition.

Motivated by the possibility that electroweak baryogenesis can be tested at future colliders, there were many proposals to realize this mechanism in extended settings [6]. Some recent attempts can be found in ref. [7]. In supersymmetric models a strong EWPT can be induced by a light top squark [8]. Supersymmetry breaking also provides new sources of CP violation. However, by now this scenario is quite constrained due to the negative Higgs searches. In the SM a lower bound of $m_H > 114\,\mathrm{GeV}$ was established [10]. A strong first order phase transition could also be driven by cubic interactions of a singlet Higgs field [9].

Recently, an alternative idea caught attention: non-renormalizable operators could have an impact on the EWPT. These operators parametrize the effects of new physics beyond some cut-off scale M. In order to be relevant at weak scale temperatures we have to assume that $M \lesssim 1\,\text{TeV}$. This new dynamics could be an ordinary quantum field theory, e.g. an extended Higgs sector. It might as well be something more fundamental, like strongly coupled gravity if the hierarchy problem is solved by the presence of extra dimensions.

If the Higgs potential is stabilized by a ϕ^6 interaction, a strong first order phase transition can occur for Higgs masses well above $100\,\text{GeV}$ [11, 12, 13]. A first order transition is triggered by a barrier in the Higgs potential. It can be provided by the one-loop thermal corrections of the weak gauge bosons. In the model under consideration, a barrier can also be generated from a negative ϕ^4 term, which no longer destabilizes the Higgs potential. The latter possibility turns out to be dominant in a large part of the parameter space. Non-renormalizable interactions also allow for new sources of the CP violation to fuel baryogenesis [14, 15].

In the following we will investigate the strengh of the EWPT in the SM with low cut-off, taking into account the one-loop corrections to the potential. At one-loop the phase transition is somewhat weaker than found in the analysis of ref. [12], where only the thermal mass part of the one-loop correction was taken into account. Still we find a strong first order EWPT for Higgs masses up to at least $170\,\text{GeV}$, if we require $M > 500\,\text{GeV}$. We will study the properties of the bubble profile, finding in particular that the wall thickness varies in a wide range from about 2 to 16 times $1/T_c$. We will discuss dimension-6 interactions between the Higgs field and the top quark which provide the necessary CP violation to fuel baryogenesis. In the WKB approximation these operators induce CP violating terms in the top quark dispersion relation which vary along the bubble wall and enter the transport equations as source terms. We will discuss novel source terms in the transport equations which enhance the generated baryon asymmetry. We find that the model can explain the observed baryon asymmetry for natural values of the parameters.

2. The strength of the phase transition

The dynamics of the EWPT is determined by the effective Higgs potential. As proposed in ref. [11], we add a non-renormalizable ϕ^6 operator to the SM potential, so that

$$V(\phi) = -\frac{\mu^2}{2}\phi^2 + \frac{\lambda}{4}\phi^4 + \frac{1}{8M^2}\phi^6 \,, \tag{2.1}$$

where $\phi^2 \equiv 2\Phi^\dagger\Phi$ with the SM Higgs doublet Φ.

At finite temperature we add a thermal mass term to the potential. Because of the positive definite ϕ^6-term, the quartic coupling λ is allowed to take negative values. In the high temperature expansion of the one-loop thermal potential we get the thermal Higgs mass term

$$\frac{1}{2}\left(\frac{1}{2}\lambda + \frac{3}{16}g_2^2 + \frac{1}{16}g_1^2 + \frac{1}{4}y_t^2\right)T^2\phi^2 \,, \tag{2.2}$$

where y_t is the top Yukawa coupling and g_2 and g_1 are the $SU(2)_L$ and $U(1)_Y$ gauge couplings. We also include the one-loop contributions due to the transverse gauge bosons

$$-\frac{g_2^3}{16\pi}T\phi^3 \tag{2.3}$$

and the top quark

$$\frac{3}{64\pi^2}y_t^4\phi^4\ln\left(\frac{Q^2}{c_F T^2}\right) \tag{2.4}$$

to the effective potential, where $c_F \approx 13.94$ [16]. We choose $Q = m_{\text{top}} = 178\,\text{GeV}$. Another choice of Q would only change the value of the self-coupling λ. Moreover we add the leading one-loop and two-loop corrections due to the ϕ^6 interaction

$$\frac{1}{8M^2}(2\phi^4 T^2 + \phi^2 T^4). \tag{2.5}$$

Altogether we end up with the high temperature effective potential

$$\begin{aligned}
V_{\text{eff}}(\phi,T) = \frac{1}{2}\left(-\mu^2 + \left(\frac{1}{2}\lambda + \frac{3}{16}g_2^2 + \frac{1}{16}g_1^2 + \frac{1}{4}y_t^2\right)T^2\right)\phi^2 - \\
-\frac{g_2^3}{16\pi}T\phi^3 + \frac{\lambda}{4}\phi^4 + \frac{3}{64\pi^2}y_t^4\phi^4\ln\left(\frac{Q^2}{c_F T^2}\right) + \\
+\frac{1}{8M^2}(\phi^6 + 2\phi^4 T^2 + \phi^2 T^4).
\end{aligned} \tag{2.6}$$

With the two conditions

$$\left.\frac{\partial V_{\text{eff}}(\phi,0)}{\partial \phi}\right|_{\phi=v} = 0 \qquad \text{and} \qquad \frac{\partial^2 V_{\text{eff}}(\phi,0)}{\partial \phi^2} = m_H^2, \tag{2.7}$$

where

$$V_{\text{eff}}(\phi,0) = V(\phi) - \frac{3}{64\pi^2}y_t^4\phi^4\ln\left(\frac{y_t^2\phi^2}{2Q^2}\right) \tag{2.8}$$

is the zero-temperature potential including the one-loop correction from the top-quark, we can express the two parameters μ and λ by the physical quantities m_H and $v = 246\,\text{GeV}$. In the following we take m_H and M as the free parameters of the model. The SM bound on the Higgs mass applies to our model, so we require $m_H > 114\,\text{GeV}$. We need $M \lesssim 1\,\text{TeV}$ in order for the dimension-six operator to be of relevance for the phase transition. If M becomes too small, for a fixed value of m_H, the electroweak minimum ceases to be the global minimum of the zero-temperature potential. As shown in figure 1, this happens around $M < 500\,\text{GeV}$, and we exclude these values from the parameter space.

During a first order phase transition there exist two energetically degenerate phases separated by an energy barrier at the critical temperature T_c. To obtain T_c and the non-zero value of the vacuum expectation value v_c the two conditions

$$\left.\frac{\partial V_{\text{eff}}(\phi,T_c)}{\partial \phi}\right|_{\phi=v_c} = 0 \qquad \text{and} \qquad V_{\text{eff}}(v_c,T_c) = 0 \tag{2.9}$$
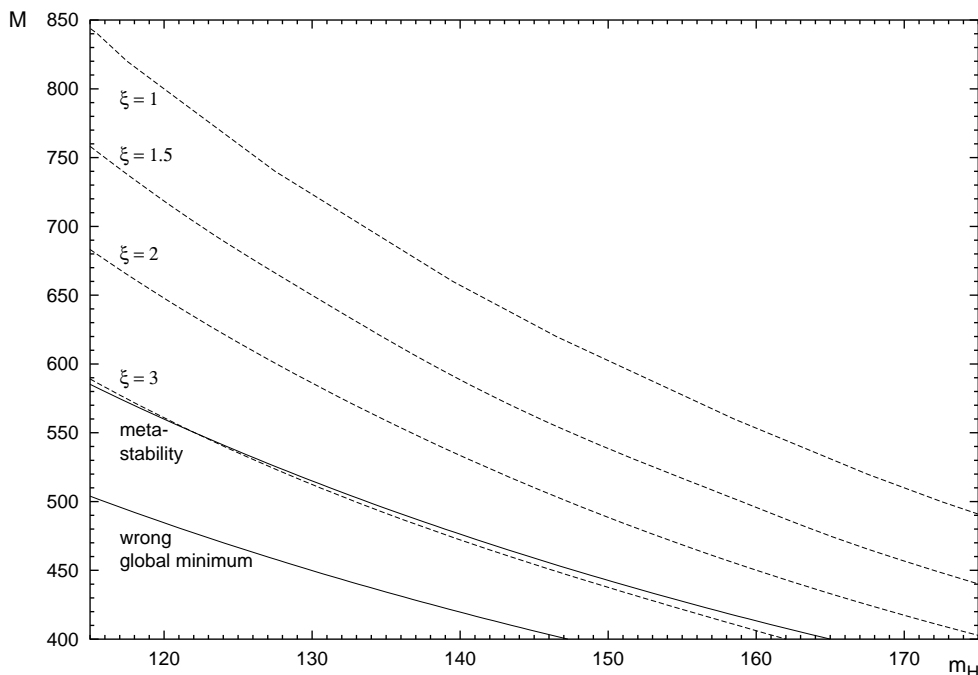
Figure 1: Contours of constant $\xi = v_c/T_c$ in the M-m_H-plane. M and m_H are given in units of GeV. Below the lowest line the zero-temperature minimum at $\phi \neq 0$ is no longer the global one. Below the metastability line the probability for thermal tunneling gets too small.

have to be fulfilled. The critical temperature in case of the EWPT is around $100\,\text{GeV}$. At some particular temperature below T_c, say T_n (nucleation temperature), the broken phase bubbles nucleate, expand and percolate. The Higgs field changes rapidly as the bubble wall passes through space. Baryogenesis has to take place outside the bubble while within the bubble the sphaleron induced $(B+L)$-violating reactions must be strongly suppressed. Otherwise the generated baryon asymmetry would be washed out after the phase transition. The sphaleron rate is practically switched off if the "washout criterion" [17]

$$\xi = \frac{v_c}{T_c} \geq 1.1 \tag{2.10}$$

is satisfied. This is the condition for a first order transition to be strong. As was discussed in ref. [12], the sphaleron energy and therefore eq. (2.10) are practically not affected by the presence of the ϕ^6 term.

In figure 1 we show the strength of the phase transition as a function of the model parameters. As expected the EWPT becomes weaker for increasing Higgs masses. For the smallest allowed Higgs mass we need $M \lesssim 825\,\text{GeV}$ to satisfy the washout criterion. In contrast to the SM we find a strongly first order phase transition, even for Higgs masses above $150\,\text{GeV}$. A large part of the parameter space meets the requirements of electroweak baryogenesis. As M approaches the region of wrong zero-temperature minimum, the critical temperature becomes smaller and ξ larger. For $\xi \gtrsim 3$ the high temperature approximation breaks down for the top quark.

What Higgs masses are compatible with the washout criterion depends on how small M is allowed to be. There is no particular bound on the ϕ^6 operator [18]. However, in figure 1 we take $M \gtrsim 400\,\text{GeV}$ in order to make an expansion in powers of v/M reasonable. In an effective field theory all operators which are allowed by the symmetries are expected to be present. In particular, we expect dimension-6 operators involving gauge fields, such as $(1/M^2)(\Phi^\dagger D_\mu \Phi)^2$. These operators have to be suppressed by a higher scale of about $10\,\text{TeV}$ in order to be in agreement with the electroweak precision data [12]. Thus a tuning of couplings on the order of $(10\,\text{TeV}/M)^2$ is required, and has to be explained by the UV completion of the model.

At the one-loop level the phase transition is somewhat weaker compared to the analysis of ref. [12]. There only the thermal masses (2.2) were included in the computation. For instance, taking $m_H = 115\,\text{GeV}$, we find $M = 825\,\text{GeV}$ to arrive at a strong enough EWPT, i.e. $\xi = 1.1$. Including only the thermal mass corrections, one arrives at $\xi = 1.43$, and the cut-off scale can be increased to about $870\,\text{GeV}$ until the phase transition becomes too weak [12].

How important are the different one-loop contributions? For $\xi \gtrsim 1$ the cubic term (2.3) is still relevant: Leaving it out considerably weakens the phase transition from $\xi = 1$ to $\xi = 0.56$, for $m_H = 115\,\text{GeV}$. Omitting also the log-term (2.4) makes the phase transition stronger again, $\xi = 0.81$. In addition, getting rid of the one-loop term of eq. (2.5) increases ξ to 1.27. Thus the one-loop contributions in (2.3)–(2.5) partially cancel each other and therefore our results agree reasonably well with those of ref. [12]. For larger Higgs masses and stronger phase transition the picture is qualitatively similar, however, the cubic term becomes less important.

The two-loop ϕ^2 term of eq. (2.5) practically does not change the result, demonstrating that the dimension-6 operator does not spoil the loop expansion. We have also checked that adding a dimension-8 term $(1/M^4)(\Phi^\dagger \Phi)^4$ only affects ξ at the order of v^2/M^2.

The one-loop effective potential was also discussed in ref. [13]. However, the authors impose an erroneous lower bound on the cut-off scale, requiring a positive mass squared for the Goldstone boson. As a result, they obtain a lower bound on the Higgs mass from eq. (2.10) which is much too small.

3. The bubble properties

In this section we discuss some bubble properties which will enter the computation of the baryon asymmetry, in particular the thickness L_w, and the velocity, v_w of the wall. As already mentioned, the two minima of V_{eff} become of the same depth at T_c, but tunneling with the formation of bubbles of the broken phase will start somewhat later at a temperature T_n. The probability for thermal tunneling is exponentially suppressed by the energy of the critical bubble, S_3. The phase transition starts if the nucleation probability per horizon volume becomes of order unity, which translates to $S_3(T_n)/T_n \sim 130 - 140$ [19].

For $\xi = 1$ the amount of supercooling, i.e. the difference between the critical and nucleation temperatures, is small. For $m_H = 115\,\text{GeV}$ we find $T_c = 107.34\,\text{GeV}$ and $T_c - T_n = 0.45\,\text{GeV}$. The system is well described by the thin wall approximation. For
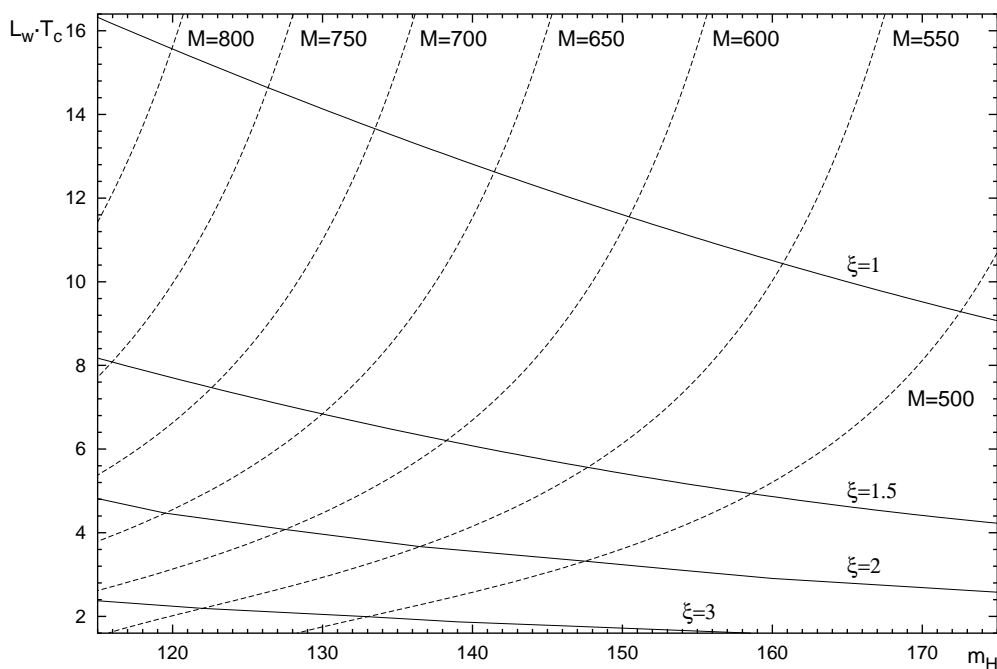
Figure 2: The wall thickness L_w as a function of the Higgs-mass m_H for several values of M, which are given in units of GeV. In addition lines of constant ξ are shown.

smaller values of M and stronger phase transition, supercooling becomes more and more important. The thin wall approximation is no longer reliable. At some critical value the phase transition does no longer proceed at all. The universe remains stuck in the symmetric vacuum. This regime is indicated by the "metastability" line in figure 1.

Once a critical bubble is nucleated it will expand. The expansion is accelerated by the internal pressure and slowed down by plasma friction. Finally, a stationary situation will be reached, where the different forces are balanced, and the wall propagates with constant velocity, v_w. In order to estimate the thickness of the bubble wall, we ignore friction for a moment and solve the field equation at the critical temperature with the effective potential of eq. (2.6),

$$\frac{d^2\phi}{dz^2} = \frac{\partial}{\partial\phi}V_{\text{eff}}(\phi).\tag{3.1}$$

The boundary conditions read $\phi(z \to -\infty) = v_c$ and $\phi(z \to \infty) = 0$. The bubble profile can approximately be described by a kink,

$$\phi(z) = \frac{v_c}{2}\left(1 - \tanh\frac{z}{L_w}\right)\tag{3.2}$$

with $L_w = \sqrt{v_c^2/(8V_b)}$, where V_b is the height of the potential barrier. This relation would be exact for a ϕ^4 potential and we found that it is also a good approximation in our case. In figure 2 the wall thickness is shown in dependence of the Higgs mass m_H and M. As we decrease M at fixed m_H, the wall thickness in units of $1/T_c$ becomes smaller. The same happens if we decrease m_H at fixed M. The main effect comes from the decrease of T_c in these cases. Notice that $L_w T_c$ varies in a wide range between about 2 and 16.

Let us finally comment on the wall velocity. Taking into account only the friction related to the infrared gauge field modes [20],

$$v_{\mathrm{w}} = \frac{32\pi L_{\mathrm{w}}}{11 g_2^2 T^3} \cdot \frac{\Delta V}{\ln(m_W L_{\mathrm{w}}) + \mathcal{O}(1)} \tag{3.3}$$

we obtain a wall velocity of order unity, except for ξ being close to one. Here ΔV is the potential difference at the nucleation temperature and m_W the mass of the W boson. The order unity correction in the denominator is induced by friction of other particles in the plasma, in particular the top quark [21]. Since numerically $\ln(m_W L_{\mathrm{w}})$ is only of order unity, top quark friction will slow down the wall considerably. The wall velocity is further reduced by latent heat of the nucleating bubbles. In general, the wall moves faster in the case of a stronger phase transition.

Let us briefly discuss two representative examples. Taking $\xi = 1$ and $m_H = 115\,\mathrm{GeV}$, we obtain $v_{\mathrm{w}} = 0.24$ from eq. (3.3). Including the effect of reheating, ΔV is reduced and we arrive at $v_{\mathrm{w}} = 0.08$. If we finally switch on the order unity correction, we end up with $v_{\mathrm{w}} \sim 0.05$. The picture looks very much different for stronger phase transitions. Going to $\xi = 1.5$, eq. (3.3) already leads to a wall velocity of order unity. Including again top quark friction and reheating, we obtain $v_{\mathrm{w}} \sim 0.5$. For larger Higgs masses we find a very similar behavior. These are only very rough estimates, since eq. (3.3) breaks down for large values of v_{w}. Given these uncertainties we will treat v_{w} as a free parameter in our computation of the baryon asymmetry.

4. CP violation

Non-renormalizable interactions provide new sources of CP violation. In the absence of gauge singlets the leading operators are of mass dimension six. In ref. [14] a $|\Phi|^2 F\tilde{F}$ operator was discussed. We will focus on the operators

$$\frac{x_{ij}^u}{M^2} (\Phi^\dagger \Phi) \Phi u_i^c q_j \tag{4.1}$$

which have been proposed to drive baryon number generation in ref. [15]. There are analogous terms for the down-type quarks and leptons. The fermion masses become

$$m_{ij} = y_{ij} \frac{v}{\sqrt{2}} + \frac{v^3}{2\sqrt{2} M^2} x_{ij} \tag{4.2}$$

where y_{ij} are the ordinary Yukawa couplings. In unitary gauge, the effective Yukawa couplings to the physical Higgs boson are given by

$$Y_{ij} = y_{ij} + \frac{3v^2}{2M^2} x_{ij} \,. \tag{4.3}$$

Thus, there is a mismatch of order (xv^2/M^2) between the fermion masses and the effective Yukawa couplings. In general, the couplings x_{ij} contain complex phases, and they are of unknown flavor structure. While for the top quark x_{33}^u may be of order unity, the couplings

of the lighter fermions should not exceed $\mathcal{O}(M^2 m_f/v^3)$ to avoid fine tuning of the fermion masses m_f. For instance, the corresponding coupling for the electron should at most be of order $10^{-4} \times (M/\text{TeV})^2$, which is a small number. Having this in mind, and lacking a theory of flavor mixing, we will therefore assume that the x_{ij} have a similar flavor structure as the corresponding Yukawa couplings, i.e. $x_{ij} \sim y_{ij}$, up to order unity coefficients. This structure could be motivated by a Froggatt-Nielsen [22] type mechanism, where the operators (4.1) and the ordinary Yukawa couplings would have the same quantum numbers.

Since the operators (4.1) do not have to be strictly aligned with the ordinary Yukawa couplings, they will induce flavor violation and CP violation. Via tree-level Higgs exchange they generate four-fermion interactions, which, for instance, affect $K - \bar{K}$ mixing. For example, the operator $(1/Q^2)(d^c s \bar{d} \bar{s}^c)$ is generated at a level of

$$\frac{1}{Q^2} \sim \frac{v^4}{M^4 m_H^2} x_{12}^d (x_{21}^d)^* . \tag{4.4}$$

For $x_{12}^d \sim m_s \sin\theta_c/v$, where m_s denotes the strange quark mass and θ_c the Cabibbo angle, we obtain roughly $Q \sim 5 \cdot 10^7 \text{GeV} \times (M/\text{TeV})^2$. At $M \gtrsim 30\,\text{TeV}$ a 2-loop contribution of order $(1/(16\pi^2)^2) x_{12}^d (x_{21}^d)^*/M^2$ becomes dominant.[1] Experimentally, these operators are constrained to be suppressed by $Q \gtrsim 10^7$ GeV, especially in the presence of CP violation. This constraint is compatible with (4.4) for $M \gtrsim 500$ GeV. Later on we will only be interested in the coupling of the top, $x_{33}^u \sim 1$. If we make the unnatural assumption that only this coupling is present, a $dd\bar{s}\bar{s}$ operator is generated at 2-loops with $Q \sim 4 \cdot 10^9 \text{GeV} \times (M/\text{TeV})^2$. In the B system the experimental bounds are even more easily satisfied.

CP violating couplings induce electric dipole moments (EDM's). The EDM of the neutron, for instance, is experimentally constrained by $d_n/e < 6.3 \cdot 10^{-26}$ cm [23]. The individual EDM's of up and down quarks should therefore be not much larger. The up quark receives the larger contribution. At one-loop we find

$$\frac{d_u}{e} \sim \frac{1}{16\pi^2} \frac{v^3 \text{Im}(x_{13}^u x_{31}^u)}{M^4} \sim 1 \cdot 10^{-26}\text{cm} \times \left(\frac{\text{TeV}}{M}\right)^2 , \tag{4.5}$$

which might be close to the experimental bound. In the second step we assumed a maximal phase and $|x_{13}^u| \sim |x_{31}^u| \sim V_{ub}$. If only the coupling x_{33}^u is present, an EDM of roughly $d_u/e \sim 5 \cdot 10^{-27}\text{cm} \times \text{Im}(x_{33}^u) \times (\text{TeV}/M)^2$ is induced at the 2-loop level [15]. Thus a coupling x_{33}^u of order unity with a large phase can be present without inducing too large flavor changing neutral currents or EDM's, even for $M \sim 300$ GeV. Other couplings also are allowed, as long as some Yukawa-like hierarchy is respected. However, experimental signals of non-standard flavor physics could be detected in the near future.

At low energies the non-renormalizable operators and the Yukawa couplings melt into the couplings (4.3). However, during the EWPT the two terms in (4.3) vary differently along the bubble wall. As a result, the fermion masses acquire position dependent phases

---

[1]This diagram is quadratically divergent which we cut off at the scale M.

which cannot be rotated away. For the phase of the top quark mass we obtain

$$\tan\theta_t(z) \approx \sin\varphi_t \frac{\phi^2(z)}{2M^2}\frac{x_t}{y_t}\,, \tag{4.6}$$

where we defined $x_t e^{i\varphi_t} \equiv x_{33}^u$ and ignored the real part of x_{33}^u. In two Higgs doublet models such a phase may arise from spontaneous CP violation. In supersymmetric models position dependent phases are induced by flavor mixing, e.g. for the charginos. In the next section we discuss how the phase (4.6) drives the generation of a baryon asymmetry as a bubble wall moves through the plasma.

5. Transport equations

The CP violating interactions of particles in the plasma with the bubble wall create an excess of left-handed quarks over the corresponding anti-quarks.[2] In the symmetric phase the left-handed quark density biases the sphaleron transitions to generate a net baryon asymmetry.

In the WKB approach the CP violating interaction of a fermion with the wall leads to different dispersion relations for particles and anti-particles [24], depending on their complex masses. To make this method applicable, it is required that the typical de Broglie wavelength of particles in the plasma is small compared to the width of the wall, i.e. $L_\mathrm{w}T \gg 1$. Otherwise an expansion in derivatives of the background Higgs field cannot be justified. According to the results of section 3 this is a good approximation in a large fraction of our parameter space. It is violated only in the cases of a very strong phase transition, $\xi \gtrsim 3$. From the dispersion relations we compute a force term which enters the transport equations that describe the evolution of the plasma. An alternative approach was followed in ref. [26].

Let us consider a single Dirac fermion, such as the top quark, with a space-time dependent mass $\mathrm{Re}\mathcal{M}(\bar{z}) + i\gamma^5\mathrm{Im}\mathcal{M}(\bar{z})$, where $\mathcal{M}(\bar{z}) = m(\bar{z})e^{i\theta(\bar{z})}$ and $\bar{z} \equiv z - v_\mathrm{w}t$ denotes the relative coordinate perpendicular to the wall. For particles and anti-particles the dispersion relations to first order in derivatives read [25]

$$E_\pm = E_0 \pm \Delta E = \sqrt{p^2 + m^2} \pm \mathrm{sign}(p_z)\theta'\frac{m^2}{2(p^2 + m^2)}\,, \tag{5.1}$$

where $p^2 = \vec{p}^2$ is the squared kinetic momentum and $\theta' = d\theta/d\bar{z}$. E_+ is the energy of left-handed particles, E_- corresponds to the right-handed states, and for the anti-particles the other way round.[3] In a more rigorous treatment similar dispersion relations were derived for spin states in the Schwinger-Keldysh formalism [27, 28].

The evolution of the particle distributions $f_i(t, \vec{x}, \vec{p})$ we describe by classical Boltzmann equations. The dispersion relations (5.1) induce force terms, which are different for particles

---

[2]Quarks will turn out to be more important than leptons because of the large top mass.

[3]Later on the relevant particles will be relativistic, so that we can approximate helicity by chirality.

and anti-particles. To make the system of equations tractable, we use a fluid-type ansatz in the rest frame of the plasma [24]

$$f_i(t, \vec{x}, \vec{p}) = \frac{1}{e^{\beta(E_i - v_i p_z - \mu_i)} \pm 1} \, , \qquad (5.2)$$

where v_i and μ_i denote velocity perturbations and chemical potentials for each fluid. The velocity perturbations are introduced to model the movement of particles in response to the force.

For a shorter notation let us first introduce some symbols K, which represent momentum averages normalized relative to the massless Fermi-Dirac case,

$$\langle X \rangle \equiv \frac{\int d^3 p \, X(p)}{\int d^3 p \, f'_+(m=0)} \, , \qquad (5.3)$$

where $f'_\pm = -\beta e^{\beta E_0}/(e^{\beta E_0} \pm 1)^2$. We define

$$K_{1,i} = \left\langle \frac{p_z^2}{\sqrt{p^2 + m_i^2}} f'_\pm(m_i) \right\rangle , \qquad K_{2,i} = \left\langle p_z^2 f'_\pm(m_i) \right\rangle ,$$

$$K_{3,i} = \left\langle \frac{1}{2\sqrt{p^2 + m_i^2}} f'_\pm(m_i) \right\rangle , \qquad K_{4,i} = \left\langle \frac{|p_z|}{2(p^2 + m_i^2)} f'_\pm(m_i) \right\rangle ,$$

$$K_{5,i} = \left\langle \frac{|p_z| p^2}{2(p^2 + m_i^2)^2} f'_\pm(m_i) \right\rangle , \qquad K_{6,i} = \left\langle \left(\frac{|p_z|}{(p^2 + m_i^2)^2} - \frac{\delta(p_z)}{p^2 + m_i^2} \right) f'_\pm(m_i) \right\rangle ,$$

$$K_{7,i} = \left\langle \frac{|p_z|^3}{(p^2 + m_i^2)^2} f'_\pm(m_i) \right\rangle , \qquad (5.4)$$

which appear in the transport equations discussed in the following. In the case of a massless fermion we obtain $K_1 = 1.096T$, $K_2 = 4.606T^2$, $K_3 = 0.211/T$, $K_4 = 0.105/T$, $K_5 = 0.105/T$, $K_6 = -0.038/T^3$ and $K_7 = 0.105/T$. For $m \gg T$ the averages experience an exponential Boltzmann suppression.

We look for solutions of the Boltzmann equation which are stationary, i.e. which only depend on the relative coordinate $\bar{z}$. We expand the Boltzmann equation in derivatives of the fermion mass. At first order in derivatives there is no difference between particles and anti-particles. Weighting the Boltzmann equation with 1 and p_z, we obtain after momentum averaging

$$\kappa_i v_\mathrm{w} \mu'_{i,1} - K_{1,i} v'_{i,1} - \langle \mathcal{C}_i \rangle = K_{3,i} v_\mathrm{w} (m_i^2)' \qquad (5.5)$$

$$- K_{1,i} \mu'_{i,1} + K_{2,i} v_\mathrm{w} v'_{i,1} - \langle p_z \mathcal{C}_i \rangle = 0 \, . \qquad (5.6)$$

Here $\mu_{i,1}$ and $v_{i,1}$ indicate the perturbations to first order in derivatives. A prime denotes again a derivative with respect to $\bar{z}$. The statistical factor $\kappa_i \equiv \langle f'_\pm(m_i) \rangle$ is 1 (2) for massless fermions (bosons) and becomes exponentially small for $m \gg T$. The force term on the right-hand side is induced by the change in the particle mass along the wall. Introducing

inelastic rates, Γ_p^{inel}, and elastic rates, Γ_p^{el}, for a process p, the collision terms take the form [29]

$$\langle \mathcal{C}_i \rangle = \sum_p \Gamma_p^{\text{inel}} \sum_j \mu_j \,, \qquad \langle p_z \mathcal{C}_i \rangle = v_i \bar{p}_z^2 \sum_p \Gamma_p^{\text{el}} \equiv v_i \bar{p}_z^2 \Gamma_i^{\text{el}} \,. \tag{5.7}$$

In $\langle p_z \mathcal{C}_i \rangle$ we neglected inelastic processes. The leading order eqs. (5.5), (5.6) contain the friction terms which enter the computation of the wall velocity [21].

To second order in derivatives, we have to distinguish between particles and anti-particles. The perturbations contain CP odd and even components,

$$\mu_i = \mu_{i,1} + \mu_{i,2o} + \mu_{i,2e} \,, \qquad v_i = v_{i,1} + v_{i,2o} + v_{i,2e} \,. \tag{5.8}$$

In the following only the odd second order perturbations will enter, so we can drop the subscript "o" to simplify the notation. Subtracting the equations of particles and anti-particles, we obtain

$$\kappa_i v_{\text{w}} \mu'_{i,2} - K_{1,i} v'_{i,2} - \langle \mathcal{C}_i \rangle = -K_{6,i} \theta'_i m_i^2 \mu'_{i,1} \tag{5.9}$$

$$-K_{1,i} \mu'_{i,2} + K_{2,i} v_{\text{w}} v'_{i,2} - \langle p_z \mathcal{C}_i \rangle = K_{4,i} v_{\text{w}} m_i^2 \theta''_i + K_{5,i} v_{\text{w}} (m_i^2)' \theta'_i - K_{7,i} m_i^2 \theta'_i v'_{i,1} \,. \tag{5.10}$$

Note that the CP violating source terms are proportional to derivatives of θ_i. A constant phase does not contribute. The source terms proportional to the first order perturbations have not been investigated so far in a realistic context. (See ref. [28] for a discussion in the context of Schwinger-Keldysh formalism.) To study their relevance for the generation of the observed baryon asymmetry will be a main issue in the next section.

We may use eq. (5.9) to solve for $v_{i,2}$. Neglecting derivatives of the thermal averages, which are higher order in derivatives, we end up with diffusion equations for the chemical potentials

$$-\kappa_i D_i (1 - A_i v_{\text{w}}^2) \mu''_{i,2} - \kappa_i v_{\text{w}} \mu'_{i,2} - D_i A_i v_{\text{w}} \sum_p \Gamma_p^{\text{inel}} \sum_j \mu'_{j,2} +$$

$$+ \sum_p \Gamma_p^{\text{inel}} \sum_j \mu_{j,2} - A_i D_i v_{\text{w}} \sum_p (\Gamma_p^{\text{inel}})' \sum_j \mu_{j,2} = S_i \,, \tag{5.11}$$

where

$$A_i = \frac{\kappa_i K_{2,i}}{K_{1,i}^2} \,. \tag{5.12}$$

In the massless limit we have $A \approx 3.83$. The diffusion constants are given by [29]

$$\kappa_i D_i = \frac{K_{1,i}^2}{\bar{p}_z^2 \Gamma_i^{\text{el}}} \,. \tag{5.13}$$

To leading order in the wall velocity, neglecting derivatives of the inelastic rates and ratios of inelastic to elastic rates, the left-hand side of eq. (5.11) reproduces the result of ref. [29]. This corresponds to dropping the terms proportional to A_i. In the next section we will examine to what extent this simplification is justified. Since A_i is not a small number,

the corrections will turn out to be important in certain regimes. For the source terms we obtain

$$S_i = \frac{\kappa_i D_i v_{\mathrm{w}}}{K_{1,i}} \left(K_{4,i} m_i^2 \theta_i'' + K_{5,i} (m_i^2)' \theta_i' \right)' +$$

$$+ K_{6,i} \left(1 - A D_i v_{\mathrm{w}} \frac{d}{d\bar{z}} \right) \left(m_i^2 \theta_i' \mu_{i,1}' \right) - \frac{\kappa_i D_i K_{7,i}}{K_{1,i}} \left(m_i^2 \theta_i' v_{i,1}' \right)'. \tag{5.14}$$

In the second line new source terms related to the first order perturbations are showing up. As expected, no source terms are left in the case of vanishing wall velocity.

Let us apply these general results to the SM with a low cut-off. In a first step we compute the asymmetry in the left-handed quark density. At this stage we neglect the weak sphalerons, i.e. baryon and lepton number are conserved. The most important particle species are the left- and right-handed top quarks and the Higgs bosons. Leptons are only produced by small Yukawa couplings and therefore not taken into account. It turns out that also the Higgs bosons have only a minor impact on the generated baryon asymmetry. They change the final result only at the percent level, so we can ignore them. In a second step, the weak sphalerons convert the left-handed quark number into a baryon asymmetry.

We take into account the top Yukawa interaction, Γ_y, the strong sphalerons, Γ_{ss} and the top helicity flips, Γ_m caused by the interactions with the bubble wall. The latter are only present in the broken phase. The gauge interactions are assumed to be in equilibrium. The transport equations become

$$(3\kappa_t + 3\kappa_b) v_{\mathrm{w}} \mu_{q3,2}' - (3K_{1,t} + 3K_{1,b}) v_{q3,2}' -$$
$$-6\Gamma_y (\mu_{q3,2} + \mu_{t,2}) - 6\Gamma_m (\mu_{q3,2} + \mu_{t,2}) -$$
$$-6\Gamma_{ss}[(2 + 9\kappa_t + 9\kappa_b)\mu_{q3,2} + (1 - 9\kappa_t)\mu_{t,2}] = -3K_{6,t} m_t^2 \theta_t' \mu_{q3,1}' \tag{5.15}$$

$$-(K_{1,t} + K_{1,b}) \mu_{q3,2}' + (K_{2,t} + K_{2,b}) v_{\mathrm{w}} v_{q3,2}' -$$
$$-\left(\frac{K_{1,t}^2}{\kappa_t D_Q} + \frac{K_{1,b}^2}{\kappa_b D_Q} \right) v_{q3,2} = K_{4,t} v_{\mathrm{w}} m_t^2 \theta_t'' + K_{5,t} v_{\mathrm{w}} (m_t^2)' \theta_t' -$$
$$- K_{7,t} m_t^2 \theta_t' v_{q3,1}' \tag{5.16}$$

$$3\kappa_t v_{\mathrm{w}} \mu_{t,2}' - 3K_{1,t} v_{t,2}' - 6\Gamma_y (\mu_{q3,2} + \mu_{t,2}) -$$
$$-6\Gamma_m (\mu_{q3,2} + \mu_{t,2}) -$$
$$-3\Gamma_{ss}[(2 + 9\kappa_t + 9\kappa_b)\mu_{q3,2} + (1 - 9\kappa_t)\mu_{t,2}] = -3K_{6,t} m_t^2 \theta_t' \mu_{t,1}' \tag{5.17}$$

$$-K_{1,t} \mu_{t,2}' + K_{2,t} v_{\mathrm{w}} v_{t,2}' - \frac{K_{1,t}^2}{\kappa_t D_Q} v_{t,2} = K_{4,t} v_{\mathrm{w}} m_t^2 \theta_t'' + K_{5,t} v_{\mathrm{w}} (m_t^2)' \theta_t' -$$
$$- K_{7,t} m_t^2 \theta_t' v_{t,1}'. \tag{5.18}$$

The top quark phase, θ_t, is given by eq. (4.6). For the chemical potentials we take $\mu_t = \mu(u_3^c)$ and $\mu_{q3} = (\mu(u_3) + \mu(d_3))/2$. The index t (b) refers to the top and bottom quark, respectively. We have omitted the tiny source of the bottom quark which is suppressed by $(m_b/m_t)^4$. We used baryon number conservation to express the strong sphaleron interaction in terms of $\mu_{q3,2}$ and $\mu_{t,2}$ [30]. Replacing the second order source terms by the first order ones, the same system of transport equation holds for the first order perturbations.

Using again baryon number conservation, the chemical potential of left-handed quarks, $\mu_{B_L} = \mu_{q_1} + \mu_{q_2} + \mu_{q_3}$, is obtained as

$$\mu_{B_L} = (1 + 2\kappa_t + 2\kappa_b)\mu_{q_3} - 2\kappa_t\mu_t \,. \tag{5.19}$$

The baryon asymmetry is then given by [25]

$$\eta_B = \frac{n_B}{s} = \frac{405\bar{\Gamma}_{ws}}{4\pi^2 v_{\mathrm{w}} g_* T^4} \int_0^\infty d\bar{z}\,\mu_{B_L}(\bar{z})e^{-\nu\bar{z}} \,, \tag{5.20}$$

where $\bar{\Gamma}_{ws}$ is the weak sphaleron rate and $\nu = 45\bar{\Gamma}_{ws}/(4v_{\mathrm{w}}T^3)$. The effective number of degrees of freedom in the plasma is $g_* = 106.75$. In eq. (5.20) the weak sphaleron rate has been suddenly switched off in the broken phase, $\bar{z} < 0$. The exponential factor in the integrand accounts for the relaxation of the baryon number if the wall moves very slowly.

6. Numerical results

In this section we present our evaluations of the transport equations (5.15)–(5.18). We will discuss under what conditions the terms proportional to A_i may be neglected in eq. (5.11) and investigate what is the impact of the new source terms in eqs. (5.9) and (5.10). Finally, we will demonstrate that the SM with a low cut-off can explain the observed baryon asymmetry for natural values of the parameters.

In our numerical computations we use the following values for the weak sphaleron rate [31], the strong sphaleron rate [32], the top Yukawa rate [30], the top helicity flip rate and the quark diffusion constant [30]

$$\bar{\Gamma}_{ws} = 1.0 \cdot 10^{-6}T^4 \,, \qquad \bar{\Gamma}_{ss} = 4.9 \cdot 10^{-4}T^4 \,,$$
$$\Gamma_y = 4.2 \cdot 10^{-3}T \,, \qquad \Gamma_m = \frac{m_t^2(\bar{z}, T)}{63T} \,,$$
$$D_Q = \frac{6}{T} \,. \tag{6.1}$$

Note that in $\bar{\Gamma}_{ss} \equiv \Gamma_{ss}T^3$ the value $\alpha_s = 0.086$ from the dimensionally reduced theory has been used [32]. Changing the rates Γ_y and Γ_m has only a small effect on the baryon asymmetry, as would have the inclusion of the Higgs field chemical potential in the transport equations. Doubling the value of D_Q enhances the baryon asymmetry by 20-30% because of more efficient diffusion. Enhancing Γ_{ss} reduces the baryon asymmetry since the strong sphalerons drive μ_{B_L} to zero if the quarks are taken massless [33]. The baryon asymmetry also depends on whether we take the top quark to be massive or massless in the thermal averages. If we switch on the top mass, the baryon asymmetry becomes smaller since the thermal averages go down. In the evaluations we use the half m_t^2 of the broken phase to compute the averages.

Let us first discuss under which conditions the A_i corrections in eq. (5.11) become important. At this stage we do not yet relate the bubble wall parameters to the model introduced in section 2. In figure 3 we display the baryon asymmetry computed with the simplified equations (dashed lines) compared to the one obtained from the full equations (5.15)–(5.18) (solid lines) as a function of the wall velocity. We take $\xi = 1.5$ and $M/T = 6$ for three different values of L_{w}. The CP violating phase in the dimension-6 oper-
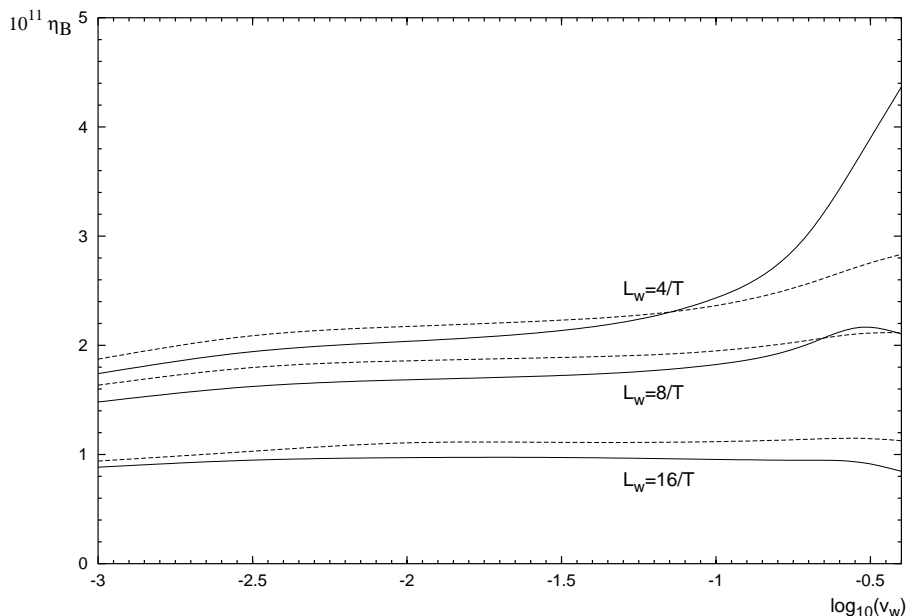
Figure 3: Comparison between eq. (5.11), where the terms proportional to A_i have been neglected (dashed), and eqs. (5.15)–(5.18) without the first order perturbations (solid) for different values of $L_{\rm w}$. The other parameters are taken as $\xi = 1.5$ and $M = 6T$.

ator (4.1) we take as maximal, i.e. $\sin\varphi_t = 1$, and we choose $x_t = 1$. In any case the baryon asymmetry is proportional to $x_t \sin\varphi_t$. Since we want to compare the left hand sides of the transport equations, we included only the source term of the first line of eq. (5.14). The simplified equations give a reasonable description for $v_{\rm w} \lesssim 0.1$. For large values of $v_{\rm w}$ there are sizable deviations, especially for thinner bubble walls. This behavior is expected since the A_i corrections come with additional powers of the wall velocity. In the MSSM, where $v_{\rm w} \sim 0.05 - 0.1$ [34], the simplified equations are applicable. In the following we will use the full equations (5.15)–(5.18) to compute the baryon asymmetry. Figure 3 also demonstrates that the baryon asymmetry increases for thinner bubble walls. This behavior is expected since the source terms involve derivatives of the background Higgs field.

In figure 4 we compare the contributions to the baryon asymmetry due to the different source terms on the right hand side of eqs. (5.9) and (5.10), using the parameters of figure 3 and $L_{\rm w} = 8/T$. The new source terms proportional to the first order perturbations $\mu_{i,1}$ and $v_{i,1}$ are non-negligible. They enhance the baryon asymmetry, especially for small values of $v_{\rm w}$. For large wall velocities they do no longer matter. The total baryon asymmetry depends only mildly on $v_{\rm w}$, which is quite positive, given our poor understanding of this parameter. For other wall widths the picture is similar.

As shown in figure 5 the baryon asymmetry increases rapidly for larger values of ξ. We fixed $v_{\rm w} = 0.01$ and 0.3 and again $L_{\rm w} = 8/T$. For large ξ the top quark mass becomes larger in the broken phase, and the source terms involve powers of m_t^2. Also the CP violating phase in the top quark mass from eq. (4.6) becomes stronger. The source terms related to the first order perturbations have an additional power of m_t^2. Therefore they grow even faster and dominate for large ξ. This behavior holds also for other values of $L_{\rm w}$.
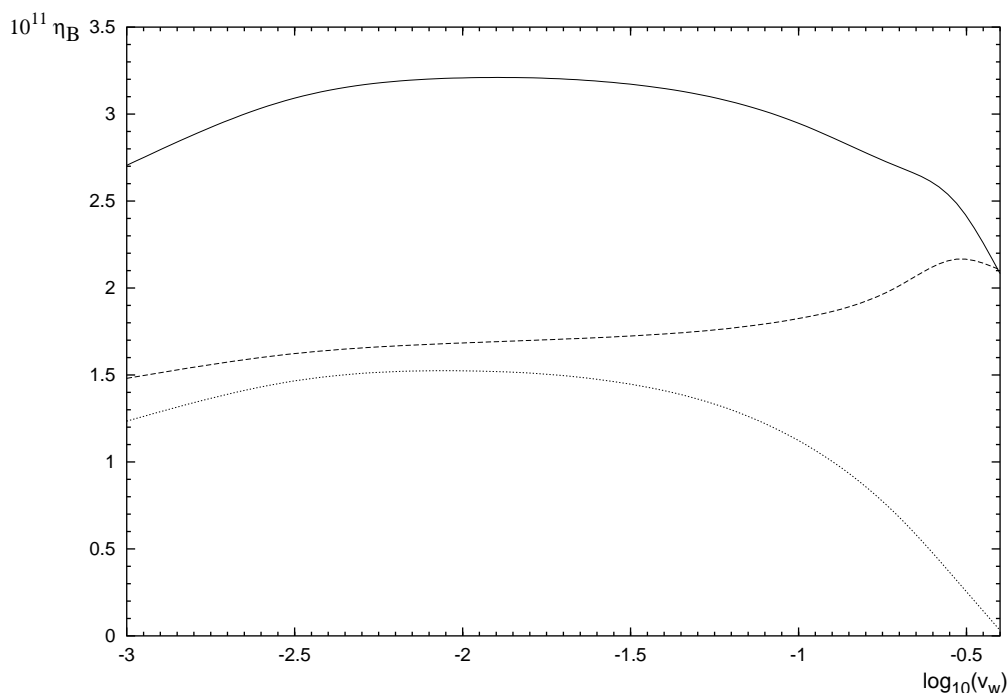
Figure 4: The solid line represents η_B as a function of the wall velocity for $L_{\rm w} = 8/T$, $M = 6T$ and $\xi = 1.5$. The dashed line would be the asymmetry without the source terms containing the first order perturbations μ_1' and v_1' and the dotted one is the contribution due to these terms only.
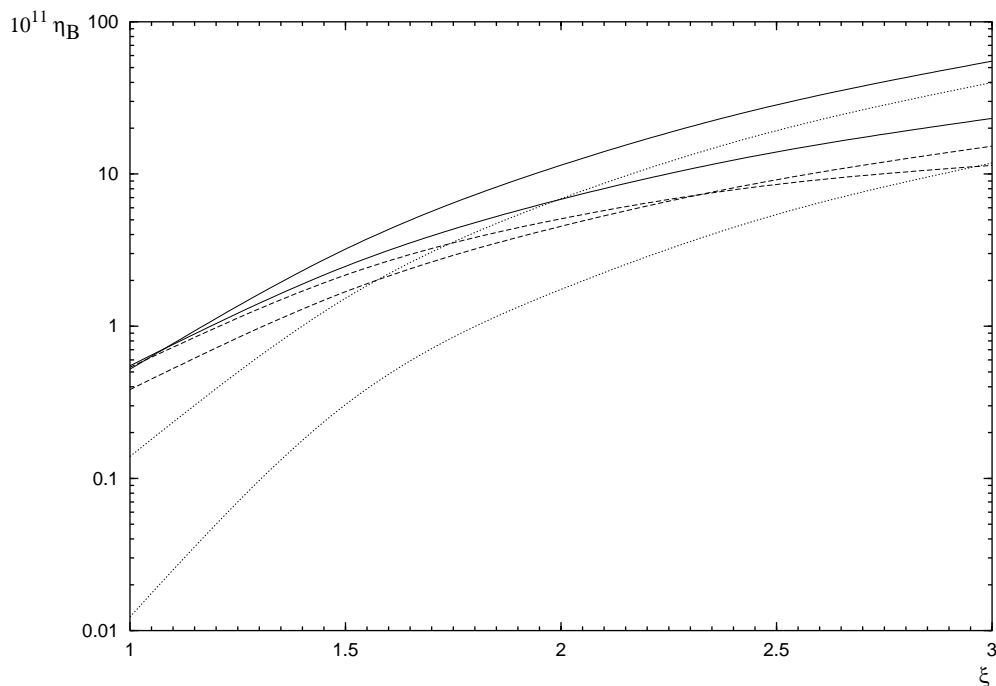
Figure 5: The baryon asymmetry as a function of ξ for two wall velocities. The different line types have the same meaning as in figure 4, and again $L_{\rm w} = 8/T$ and $M = 6T$. On the right edge of the figure the upper curves are for $v_{\rm w} = 0.01$ and the lower ones for $v_{\rm w} = 0.3$.
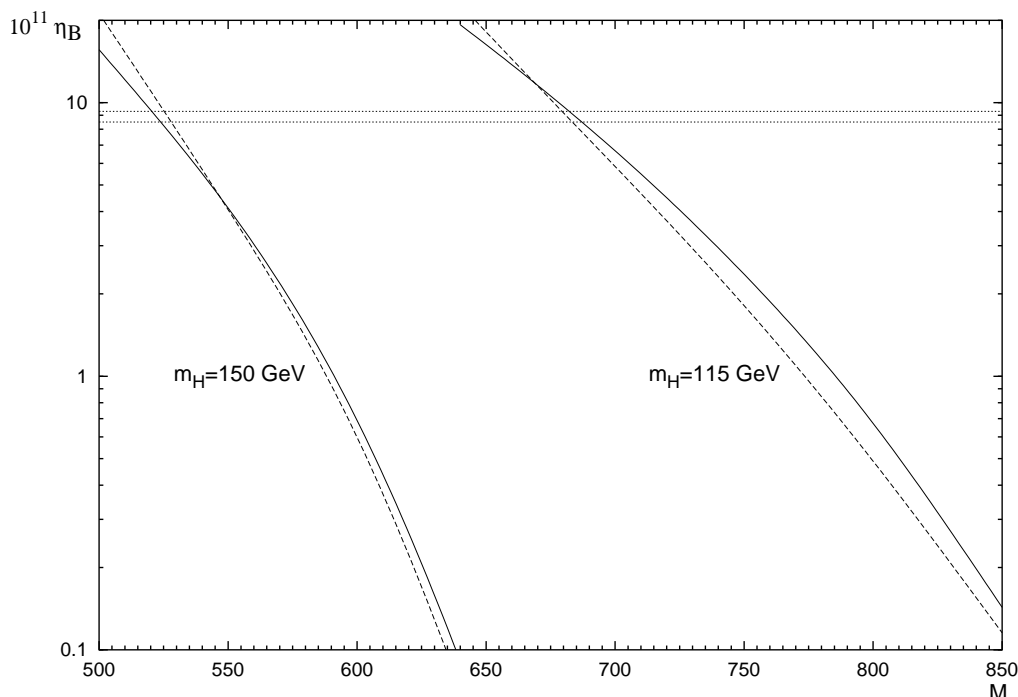
Figure 6: The baryon asymmetry in the SM with low cut-off for two different Higgs masses as a function of M (in units of GeV) for $v_{\rm w} = 0.01$ (solid) and $v_{\rm w} = 0.3$ (dashed). The horizontal lines indicate the errorband of the measured value.

Let us finally relate the bubble wall parameters to our SM with low cut-off. In the figure 6 we present the baryon asymmetry in the model for $m_H = 115$ and $150\,\text{GeV}$ as a function of the cut-off scale M. For every value of M we compute the strength of the phase transition and the bubble width. We consider one small $v_{\rm w} = 0.01$ and one large wall velocity $v_{\rm w} = 0.3$. We take again a maximal CP violating phase $\sin\varphi_t = 1$ and $x_t = 1$. As expected the baryon asymmetry grows rapidly as we lower M. At the very lowest values of M the wall thickness becomes of order $1/T$ (see figure 2) so that our WKB approach ceases to be reliable. Moreover, the bubble walls may become relativistic in this regime, and diffusion of charges into the symmetric phase may no longer be efficient. One can see that η_B depends only mildly on the wall velocity.

Nevertheless, independent of the Higgs mass we have chosen, we can generate the observed baryon asymmetry (1.1) without amplifying the CP violating dimension-6 operator (4.1). This requires the phase transition to be sufficiently strong, i.e. $\xi \gtrsim 1.5$. At this strength of the phase transition our computation of the baryon asymmetry is still under control. For smaller values of ξ we have to take $x_t > 1$. For instance, in the case of $m_H = 115\,\text{GeV}$ and $\xi = 1.1$ ($M = 825\,\text{GeV}$), we could use $x_t \sim 40$ which is barely consistant with the bound from the neutron EDM discussed in section 3. Thus the SM with low cut-off can account for the observed baryon asymmetry in a wide range of the model parameters, without being in conflict with constraints from flavor and CP violation.

At the end of this section let us briefly comment on the impact of sources from the bottom quark and the tau lepton. In case of the bottom the source term is heavily sup-

pressed by $(m_b/m_t)^4 \sim 10^{-7}$. The tau lepton is more relevant because of its larger diffusion constant of about $380/T$ [35]. Still its contribution is about 10^5 times smaller than that of the top quark and can be safely neglected.

7. Conclusions

We have investigated the electroweak phase transition and baryogenesis in the standard model augmented by a dimension-6 Higgs self interaction. Taking the suppression scale of this operator to be $M \lesssim 1\,\mathrm{TeV}$, the EWPT becomes first order, without introducing new degrees of freedom in the model. In addition to the Higgs mass only the parameter M enters the computation of the phase transition. There is no relevant bound on the ϕ^6 interaction. However, dimension-6 operators involving for instance gauge fields, which are also expected to be present in a general effective field theory, have to be tuned at the level of 10^{-2} in order not to spoil the electroweak fit [12].

Requiring $M > 500\,\mathrm{GeV}$ the phase transition is strong enough to prevent baryon number washout for Higgs masses up to $170\,\mathrm{GeV}$. In our analysis we have used the one-loop thermal potential. The phase transition is somewhat weaker than found in ref. [12], where only the thermal mass part of the one-loop correction was taken into account. We have checked that the dimension-6 operator does not spoil the loop expansion of the effective potential. We have computed the wall thickness which turns out to vary in a wide range from about $2/T$ to $16/T$. As M becomes smaller the EWPT becomes stronger and the bubble wall thinner. For very small cut-off scales the symmetric phase becomes metastable.

A dimension-6 operator involving the Higgs field and the top quark provides a new source of CP violation. It induces a complex phase in the top quark mass which varies along the phase boundary. We discussed that this operator is consistent with present bounds on EDM's and flavor violation for $M \gtrsim 300\,\mathrm{GeV}$. However, it may leave a detectable signal in forthcoming experiments.

As a result of the varying phase, top quarks and anti-top quarks experience a different force as they pass through the bubble wall. We treat the system in the WKB approximation, expanding in derivatives of the background Higgs field. Our approach is valid for a large fraction of the parameter space of the model. It will break down for very small values of the cut-off scale M, where the bubble width becomes of order the inverse temperature. The CP violating force enters the transport equations which describe the hot plasma. Carefully expanding in derivatives of the wall profile, we find novel source terms which enhance the generated baryon asymmetry. They are especially relevant for slow bubble walls and dominate over the known source terms for large values of the particle mass. Because of these properties they should play a prominent role in the MSSM, where the top quark is replaced by the charginos.

In the model considered, the observed baryon asymmetry can be explained for natural values of the parameters. The phase transition should be somewhat stronger than required by the washout criterion. If the EWPT is not that strong, the coefficient of the CP violating dimension-6 operator has to be taken larger than one, which is compatible

with experiments. It would also be interesting to study the impact of other CP violating operators, such as the one discussed in ref. [14], which has been ignored in our study.

With a low cut-off the model is expected to lead to non-standard signals in flavor physics, such as EDM's and flavor changing neutral currents, which can be tested in future experiments. The LHC will be able to directly test the physics at the cut-off scale. If the general cut-off scale is in the multi-TeV range and the ϕ^6 interaction is anomalously large, the model could still be identified by its non-standard Higgs self couplings. However, the required precision will probably take a linear collider [12].

In conclusion, the standard model with low cut-off provides the missing ingredients for electroweak baryogenesis: a strong phase transition and additional CP violation. Moreover, its simple structure makes it an ideal laboratory to refine the computation of the baryon asymmetry.

Acknowledgments

References

[1] WMAP collaboration, D.N. Spergel *et al.*, *First year wilkinson microwave anisotropy probe (wmap) observations: determination of cosmological parameters*, *Astrophys. J. Suppl.* **148** (2003) 175 [`astro-ph/0302209`].

[2] SDSS collaboration, M. Tegmark *et al.*, *Cosmological parameters from SDSS and WMAP*, *Phys. Rev.* **D 69** (2004) 103501 [`astro-ph/0310723`].

[3] V.A. Kuzmin, V.A. Rubakov and M.E. Shaposhnikov, *On the anomalous electroweak baryon number nonconservation in the early universe*, *Phys. Lett.* **B 155** (1985) 36.

[4] M.B. Gavela, P. Hernandez, J. Orloff, O. Pene and C. Quimbay, *Standard model CP-violation and baryon asymmetry, part 2. Finite temperature*, *Nucl. Phys.* **B 430** (1994) 382 [`hep-ph/9406289`];
P. Huet and E. Sather, *Electroweak baryogenesis and standard model CP-violation*, *Phys. Rev.* **D 51** (1995) 379 [`hep-ph/9404302`];
T. Konstandin, T. Prokopec and M.G. Schmidt, *Axial currents from CKM matrix CP-violation and electroweak baryogenesis*, *Nucl. Phys.* **B 679** (2004) 246 [`hep-ph/0309291`].

[5] K. Kajantie, M. Laine, K. Rummukainen and M.E. Shaposhnikov, *Is there a hot electroweak phase transition at $m_H \gtrsim m_W$?*, *Phys. Rev. Lett.* **77** (1996) 2887 [`hep-ph/9605288`]; *A non-perturbative analysis of the finite t phase transition in* $SU(2) \times U(1)$ *electroweak theory*, *Nucl. Phys.* **B 493** (1997) 413 [`hep-lat/9612006`];
F. Csikor, Z. Fodor and J. Heitger, *Endpoint of the hot electroweak phase transition*, *Phys. Rev. Lett.* **82** (1999) 21 [`hep-ph/9809291`].

[6] For a review, see: A. Riotto and M. Trodden, *Recent progress in baryogenesis*, *Ann. Rev. Nucl. Part. Sci.* **49** (1999) 35–75 [`hep-ph/9901362`].

[7] S. Kanemura, Y. Okada and E. Senaha, *Electroweak baryogenesis and quantum corrections to the triple Higgs boson coupling*, `hep-ph/0411354`;
S.W. Ham, Y.S. Jeong and S.K. Oh, *Electroweak phase transition in an extension of the standard model with a real Higgs singlet*, `hep-ph/0411352`;
S.W. Ham, S.K. Oh and D. Son, *Electroweak phase transition in the MSSM with four generations*, *Phys. Rev.* **D 71** (2005) 015001 [`hep-ph/0411012`];
M. Carena, A. Megevand, M. Quiros and C.E.M. Wagner, *Electroweak baryogenesis and new TeV fermions*, `hep-ph/0410352`;
A. Menon, D.E. Morrissey and C.E.M. Wagner, *Electroweak baryogenesis and dark matter in the nmssm*, *Phys. Rev.* **D 70** (2004) 035005 [`hep-ph/0404184`].

[8] M. Carena, M. Quiros and C.E.M. Wagner, *Opening the window for electroweak baryogenesis*, *Phys. Lett.* **B 380** (1996) 81 [`hep-ph/9603420`];
D. Bodeker, P. John, M. Laine and M.G. Schmidt, *The 2-loop MSSM finite temperature effective potential with stop condensation*, *Nucl. Phys.* **B 497** (1997) 387 [`hep-ph/9612364`];
B. de Carlos and J.R. Espinosa, *The baryogenesis window in the MSSM*, *Nucl. Phys.* **B 503** (1997) 24 [`hep-ph/9703212`];
M. Laine and K. Rummukainen, *The MSSM electroweak phase transition on the lattice*, *Nucl. Phys.* **B 535** (1998) 423 [`hep-lat/9804019`].

[9] M. Pietroni, *The electroweak phase transition in a nonminimal supersymmetric model*, *Nucl. Phys.* **B 402** (1993) 27 [`hep-ph/9207227`];
A.T. Davies, C.D. Froggatt and R.G. Moorhouse, *Electroweak baryogenesis in the next to minimal supersymmetric model*, *Phys. Lett.* **B 372** (1996) 88 [`hep-ph/9603388`];
S.J. Huber and M.G. Schmidt, *SUSY variants of the electroweak phase transition*, *Eur. Phys. J.* **C 10** (1999) 473 [`hep-ph/9809506`]; *Electroweak baryogenesis: concrete in a SUSY model with a gauge singlet*, *Nucl. Phys.* **B 606** (2001) 183 [`hep-ph/0003122`];
M. Bastero-Gil, C. Hugonie, S.F. King, D.P. Roy and S. Vempati, *Does lep prefer the NMSSM?*, *Phys. Lett.* **B 489** (2000) 359 [`hep-ph/0006198`].

[10] LEP collaboration, *A combination of preliminary electroweak measurements and constraints on the standard model*, `hep-ex/0312023`.

[11] X.-m. Zhang, *Operators analysis for Higgs potential and cosmological bound on Higgs mass*, *Phys. Rev.* **D 47** (1993) 3065 [`hep-ph/9301277`].

[12] C. Grojean, G. Servant and J.D. Wells, *First-order electroweak phase transition in the standard model with a low cutoff*, `hep-ph/0407019`.

[13] S.W. Ham and S.K. Oh, *Electroweak phase transition in the standard model with a dimension-six Higgs operator at one-loop level*, *Phys. Rev.* **D 70** (2004) 093007 [`hep-ph/0408324`].

[14] M. Dine, P. Huet, J. Singleton, Robert and L. Susskind, *Creating the baryon asymmetry at the electroweak phase transition*, *Phys. Lett.* **B 257** (1991) 351.

[15] X. Zhang, S.K. Lee, K. Whisnant and B.L. Young, *Phenomenology of a nonstandard top quark yukawa coupling*, *Phys. Rev.* **D 50** (1994) 7042 [`hep-ph/9407259`].

[16] L. Dolan and R. Jackiw, *Symmetry behavior at finite temperature*, *Phys. Rev.* **D 9** (1974) 3320.

[17] G.D. Moore, *Measuring the broken phase sphaleron rate nonperturbatively*, *Phys. Rev.* **D 59** (1999) 014503 [`hep-ph/9805264`].

[18] V. Barger, T. Han, P. Langacker, B. McElrath and P. Zerwas, *Effects of genuine dimension-six Higgs operators*, *Phys. Rev.* **D 67** (2003) 115001 [`hep-ph/0301097`].

[19] G.W. Anderson and L.J. Hall, *The electroweak phase transition and baryogenesis*, *Phys. Rev.* **D 45** (1992) 2685;
for a non-perturbative treatment of bubble nucleation, see G.D. Moore and K. Rummukainen, *Electroweak bubble nucleation, nonperturbatively*, *Phys. Rev.* **D 63** (2001) 045002 [`hep-ph/0009132`].

[20] G.D. Moore, *Electroweak bubble wall friction: analytic results*, *J. High Energy Phys.* **03** (2000) 006 [`hep-ph/0001274`].

[21] G.D. Moore and T. Prokopec, *How fast can the wall move? a study of the electroweak phase transition dynamics*, *Phys. Rev.* **D 52** (1995) 7182 [`hep-ph/9506475`].

[22] C.D. Froggatt and H.B. Nielsen, *Hierarchy of quark masses, Cabibbo angles and CP-violation*, *Nucl. Phys.* **B 147** (1979) 277.

[23] P.G. Harris *et al.*, *New experimental limit on the electric dipole moment of the neutron*, *Phys. Rev. Lett.* **82** (1999) 904.

[24] M. Joyce, T. Prokopec and N. Turok, *Electroweak baryogenesis from a classical force*, *Phys. Rev. Lett.* **75** (1995) 1695 [`hep-ph/9408339`]; *Nonlocal electroweak baryogenesis, part 2. The classical regime*, *Phys. Rev.* **D 53** (1996) 2958 [`hep-ph/9410282`].

[25] J.M. Cline and K. Kainulainen, *A new source for electroweak baryogenesis in the MSSM*, *Phys. Rev. Lett.* **85** (2000) 5519 [`hep-ph/0002272`];
J.M. Cline, M. Joyce and K. Kainulainen, *Supersymmetric electroweak baryogenesis*, *J. High Energy Phys.* **07** (2000) 018 [`hep-ph/0006119`], erratum [`hep-ph/0110031`].

[26] M. Carena, J.M. Moreno, M. Quiros, M. Seco and C.E.M. Wagner, *Supersymmetric CP-violating currents and electroweak baryogenesis*, *Nucl. Phys.* **B 599** (2001) 158 [`hep-ph/0011055`];
M. Carena, M. Quiros, M. Seco and C.E.M. Wagner, *Improved results in supersymmetric electroweak baryogenesis*, *Nucl. Phys.* **B 650** (2003) 24 [`hep-ph/0208043`].

[27] K. Kainulainen, T. Prokopec, M.G. Schmidt and S. Weinstock, *First principle derivation of semiclassical force for electroweak baryogenesis*, *J. High Energy Phys.* **06** (2001) 031 [`hep-ph/0105295`]; *Semiclassical force for electroweak baryogenesis: three-dimensional derivation*, *Phys. Rev.* **D 66** (2002) 043502 [`hep-ph/0202177`].

[28] T. Prokopec, M.G. Schmidt and S. Weinstock, *Transport equations for chiral fermions to order h-bar and electroweak baryogenesis*, *Ann. Phys. (NY)* **314** (2004) 208 [`hep-ph/0312110`]; *Transport equations for chiral fermions to order h-bar and electroweak baryogenesis, II*, *Ann. Phys. (NY)* **314** (2004) 267 [`hep-ph/0406140`].

[29] J.M. Cline, M. Joyce and K. Kainulainen, *Supersymmetric electroweak baryogenesis in the wkb approximation*, *Phys. Lett.* **B 417** (1998) 79 [`hep-ph/9708393`].

[30] P. Huet and A.E. Nelson, *Electroweak baryogenesis in supersymmetric models*, *Phys. Rev.* **D 53** (1996) 4578 [`hep-ph/9506477`].

[31] G.D. Moore, *Sphaleron rate in the symmetric electroweak phase*, *Phys. Rev.* **D 62** (2000) 085011 [`hep-ph/0001216`]; *Do we understand the sphaleron rate?*, `hep-ph/0009161`; *The sphaleron rate: boedeker's leading log*, *Nucl. Phys.* **B 568** (2000) 367 [`hep-ph/9810313`];

P. Arnold and L.G. Yaffe, *High temperature color conductivity at next-to-leading log order*, *Phys. Rev.* **D 62** (2000) 125014 [`hep-ph/9912306`];

D. Bodeker, *On the effective dynamics of soft non-abelian gauge fields at finite temperature*, *Phys. Lett.* **B 426** (1998) 351 [`hep-ph/9801430`].

[32] G.D. Moore, *Computing the strong sphaleron rate*, *Phys. Lett.* **B 412** (1997) 359 [`hep-ph/9705248`].

[33] G.F. Giudice and M.E. Shaposhnikov, *Strong sphalerons and electroweak baryogenesis*, *Phys. Lett.* **B 326** (1994) 118 [`hep-ph/9311367`].

[34] P. John and M.G. Schmidt, *Do stops slow down electroweak bubble walls?*, *Nucl. Phys.* **B 598** (2001) 291 [`hep-ph/0002050`], erratum *ibid.* **648** (2003) 449

[35] M. Joyce, T. Prokopec and N. Turok, *Nonlocal electroweak baryogenesis, part 1. Thin wall regime*, *Phys. Rev.* **D 53** (1996) 2930 [`hep-ph/9410281`].